J|A|C|S
ARTICLES
Published on Web 12/05/2003

# β-Octafluorocorroles

Erik Steene, Abhishek Dey,† and Abhik Ghosh*

*Contribution from the Department of Chemistry, University of Tromsø, N-9037 Tromsø, Norway*

Received September 6, 2002; E-mail: abhik@chem.uit.no

***Abstract:*** The one-pot corrole synthesis first reported by the Gross and Paolesse groups appears to have evolved into a remarkably general and predictable self-assembly based synthetic reaction. Gross's solvent-free procedure (refs 8 and 9) has proven particularly effective in our hands and, in fact, more general than originally claimed. In earlier work (ref 17), we showed that the reaction works for a variety of aromatic aldehyde starting materials and was not limited to relatively electron-deficient aldehydes, as reported by Gross and co-workers. Here, we show that the pyrrole component is also variable in that 3,4-difluoropyrrole undergoes oxidative condensation with four different *p*-X-substituted benzaldehydes to yield the corresponding β-octafluoro-*meso*-tris(*para*-X-phenyl)corroles (X = $CF_3$, H, $CH_3$, and $OCH_3$). Further, we have prepared the Cu and FeCl derivatives of the β-octafluorocorrole ligands. The XPS nitrogen 1s ionization potentials of these fluorinated ligands are some 0.7 eV higher than those of the corresponding β-unfluorinated ligands. The oxidation half-wave potentials of the Cu and FeCl complexes of the fluorinated corroles are also positively shifted by 300−400 mV relative to their β-unsubstituted analogues, demonstrating the strongly electron-deficient character of the fluorinated ligands. $^1$H NMR spectroscopy suggests that like their β-unfluorinated counterparts, the new β-octafluorinated triarylcorroles act as substantially noninnocent ligands, i.e., exhibit corrole π-cation radical character, in the FeCl complexes. Quantitatively, however, NMR spectroscopy and DFT calculations indicate that the β-octafluorinated corroles are somewhat less noninnocent (i.e., carry less radical character) than their β-unfluorinated counterparts in the FeCl complexes. Temperature-dependent $^{19}$F NMR spectroscopy suggests that the Cu octafluorocorroles have a thermally accessible paramagnetic excited state, which we assign as a Cu(II) corrole π-cation radical. We have previously reported that the electronic absorption spectra, particularly the Soret absorption maxima, of high-valent transition metal triarylcorroles are very sensitive to the nature of the substituents in the *meso* positions. In contrast, the Soret absorption maxima of free-base triarylcorroles are not particularly sensitive to the nature of the *meso* substituents. This scenario also holds for the fluorinated corroles described here. Thus, although the four free-base fluorinated triarylcorroles exhibit practically identical Soret absorption maxima, the Soret bands of the Cu derivatives of the same corroles red-shift by approximately 35 nm on going from the *p*-$CF_3$ to the *p*-$OCH_3$ derivative.

## Introduction

Long known as the classic one-pot route to porphyrins,[1] the oxidative condensation of pyrrole and aromatic aldehydes[2] has also been found to yield *N*-confused porphyrins,[3−6] sapphyrins,[7] corroles,[8−11] and various expanded porphyrins.[12,13] Of these macrocycles, the *N*-confused porphyrins and particularly the corroles have exhibited an extensive coordination chemistry.[2,5,14] In particular, the trianionic corrole ligands appear to stabilize a wide variety of high-valent transition metal ions.[15] In the late 1990s, the Gross and Paolesse groups reported one-pot syntheses of *meso*-triarylcorroles.[8,10] Gross reported a solvent-free procedure for the synthesis of corroles with electron-withdrawing *meso* substituents such as *meso*-tris(pentafluorophenyl)corrole, *meso*-tris(2,6-dichlorophenyl)corrole, and *meso*-tris(heptafluorobutyl)corrole.[16] In our hands,[17] Gross's procedure turned out to be more general than originally claimed and yielded *meso*-triarylcorroles from a variety of aromatic aldehydes as starting

† Current address: Department of Chemistry, Stanford University, Stanford, CA 94305.

(1) Lindsey, J. S.; Schreiman, I. C.; Hsu, H. C.; Kearney, P. C.; Marguerettaz, A. M. *J. Org. Chem.* **1987**, *52*, 827.
(2) For a minireview on pyrrole-aldehyde condensations viewed as self-assembly processes, see: Ghosh, A. *Angew. Chem., Int. Ed.*, in press.
(3) Chmielewski, P. J.; Latos-Grazynski, L.; Rachlewicz, K.; Glowiak, T. *Angew. Chem., Int. Ed. Engl.* **1994**, *33*, 779.
(4) Furuta, H.; Asano, T.; Ogawa, T. *J. Am. Chem. Soc.* **1994**, *116*, 767.
(5) Chmielewski, P. J.; Latos-Grazynski, L. *Inorg. Chem.* **1997**, *36*, 840.
(6) Geier, G. R., III; Haynes, D. M.; Lindsey, J. S. *Org. Lett.* **1999**, *1*, 1455.
(7) Chmielewski, P. J.; Latos-Grazynski, L.; Rachlewicz, K. *Chem. Eur. J.* **1995**, *1*, 68.
(8) Gross, Z.; Galili, N.; Saltsman, I. *Angew. Chem., Int. Ed.* **1999**, *38*, 1427.
(9) Gross, Z.; Galili, N.; Simkhovich, L.; Saltsman, I.; Botoshansky, M.; Bläser, D.; Boese, R.; Goldberg, I. *Org. Lett.* **1999**, 599.
(10) Paolesse, R.; Mini, S.; Sagone, F.; Boschi, T.; Jaquinod, L.; Nurco, D. J.; Smith, K. M. *Chem. Commun.* **1999**, *14*, 1307.
(11) Paolesse, R.; Nardis, S.; Sagone, F.; Khoury, R. G. *J. Org. Chem.* **2001**, *66*, 550.
(12) Shin, J.-Y.; Furuta, H.; Yoza, K.; Igarashi, S.; Osuka, A. *J. Am. Chem. Soc.* **2001**, *123*, 7190.
(13) Shimizu, S.; Shin, J.-Y.; Furuta, H.; Ismael, R.; Osuka, A. *Angew. Chem., Int. Ed.* **2003**, *42*, 78.
(14) Nilsen, H. J.; Ghosh, A. *Acta Chem. Scand.* **1998**, *52*, 827.
(15) Erben, C.; Will, S.; Kadish, K. M. In *The Porphyrin Handbook*; Kadish, K. M., Smith, K. M., Guilard, R., Eds.; Academic Press: San Diego, 2000; Vol. 2, p 233.
(16) Simkhovich, L.; Goldberg, I.; Gross, Z. *J. Inorg. Biochem.* **2000**, *80*, 235.
(17) Wasbotten, I. H.; Wondimagegn, T.; Ghosh, A. *J. Am. Chem. Soc.* **2002**, *124*, 8104.


**10.1021/ja021158h CCC: $25.00** 

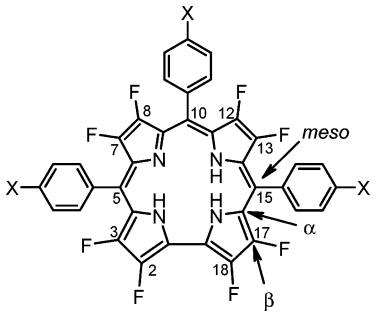


***Figure 1.*** Free-base β-octafluoro-*meso*-tris(*p*-X-phenyl)corrole (X = $OCH_3$, $CH_3$, H, and $CF_3$) ligands prepared in this work.

materials. We wished to determine whether the pyrrole fragment could also be varied in this reaction, and based on the fact that 3,4-difluoropyrrole has been successfully condensed with certain aromatic aldehydes to yield β-octafluoro-*meso*-tetraarylporphyrins[18] and, very recently, β-perfluorinated expanded porphyrins,[13] we proceeded to investigate the reactivity of 3,4-difluoropyrrole vis-à-vis the one-pot solvent-free corrole synthesis. This turned out to be a successful experiment, and we report here the synthesis of a series of four β-octafluoro-tris(*p*-X-phenyl)corroles (X = $CF_3$, H, $CH_3$, and $OCH_3$) (Figure 1).[19] The one-pot corrole synthesis may be viewed as a seven-component self-assembly process, involving three aldehydes and four pyrrole units, and it is gratifying that it seems to be robust with respect to variations in both the aldehyde and pyrrole components.[2]

Corroles generally exhibit significantly lower oxidation potentials than analogous porphyrin derivatives.[15] For example, the first half-wave potential for oxidation of Sn(OEC)Cl is 0.67 V compared to 1.36 V (vs SCE) for $Sn(OEP)Cl_2$ (OEC = β-octaethylcorrole and OEP = β-octaethylporphyrin).[15] An important question considered in the recent literature concerns how corroles, with such low oxidation half-wave potentials, can stabilize high-valent transition metal ions. Using NMR spectroscopy, DFT calculations, as well as electrochemical arguments, Walker and co-workers[20−23] and we[24−26] have shown that the corrole ligand is noninnocent, i.e., exhibits corrole π-cation radical character, in many high-valent transition metal complexes. In contrast, recent DFT calculations by Tangen and Ghosh[27] suggest that the corrolazine[28] ligand, which may be regarded as a strongly electron-deficient version of corrole, serves as a more innocent ligand, compared with corrole. Thus, the question—in fact, the one that partially led to our undertaking this project—arises as to whether an electron-deficient corrole ligand such as a β-octafluorocorrole should generally serve as a noninnocent ligand like ordinary corroles or act as a relatively innocent one like corrolazine.[27] On the basis of NMR spectroscopy, electrochemical measurements, and DFT calculations we conclude that the β-octafluorocorroles reported here, like the β-unsubstituted corroles studied previously,[20−22,24−26] indeed act as noninnocent ligands, i.e., exhibit corrole π-cation radical character, in the FeCl complexes.

## Experimental Section

**General Comments.** All samples for NMR analysis were prepared in 5 mm NMR tubes using $CDCl_3$ as solvent. A small drop of trifluoroacetic acid was added to all free-base corrole NMR samples to protonate the corrole and thereby to generate a symmetrical macrocycle comparable to the metal complexes. Unless otherwise mentioned, $^1H$ and $^{19}F$ NMR spectra were recorded with a Varian 400 MHz spectrometer at 298 K. The $^1H$ NMR spectra were referenced to residual $CHCl_3$ (δ 7.24 ppm), whereas the $^{19}F$ chemical shifts were referenced to trifluoroacetic acid (δ −76.2 ppm) for the free-base corroles and to 2,2,2-trifluoroethanol-$d_3$ (δ −77.8 ppm) for the Cu and FeCl corrole derivatives.

Cyclic voltammetry was carried out using an EG&G Model 263A Potensiostat with a three-electrode system consisting of a glassy carbon working electrode, a platinum wire counter electrode, and a saturated calomel reference electrode (SCE). Tetra(*n*-butyl)ammonium perchlorate (TBAP), recrystallized from ethanol and dried in a desiccator for at least one week, was used as the supporting electrolyte. Dichloromethane, distilled from calcium hydride and stored over molecular sieves, was used as the solvent for the cyclic voltammetry experiments. The reference electrode was separated from the bulk solution by a fritted-glass bridge filled with the solvent/supporting electrolyte mixture and all half-wave potentials reported here are referenced to the SCE. Pure argon was bubbled though solutions containing the metallocorroles for at least 2 min prior to the cyclic voltammetry experiments and the solutions were also protected from air by an argon blanket during the experiments.

X-ray photoelectron spectra were acquired at room temperature with a Physical Electronics Quantum 2000 spectrometer, equipped with a hemispherical analyzer, and 350 W of monochromatized Al Kα radiation. Sample preparation consisted of rubbing a tiny speck of the corrole into a thin film on gold foil. The films, which appeared as a colored sheen on gold, were so thin that they showed no evidence of charging in the course of X-ray bombardment. Flooding the samples with low-energy electrons did not change the positions or shapes of the XPS peaks, again proving the absence of sample charging. The binding energies reported here were externally referenced to the Au $4f_{7/2}$ binding energy (84.0 eV) of the gold substrate and were reproducible to ±0.1 eV. A full analysis of the XPS results will be presented elsewhere; in this paper, we will only discuss the XPS of the free-base fluorinated corroles.

UV−visible spectra were recorded with an HP 8453 spectrophotometer in $CH_2Cl_2$. Column chromatography was performed on Matrex 35−70 μ silica from Millipore. Elemental Analyses were conducted by Analytische Laboratorien (Prof. Dr. H. Malissa und G. Reuter GmbH), Lindlar, Germany.

**Synthesis of 3,4-Difluoropyrrole.** 3,4-Difluoropyrrole was synthesized using a slightly modified version of the procedure reported by DiMagno and co-workers.[29] The difference relative to the published

(18) Woller, E. K.; DiMagno, S. G. *J. Org. Chem.* **1997**, *62*, 1588.
(19) We should note that with pentafluorobenzaldehyde and 3,4-difluoropyrrole we did not succeed in isolating corrole products under the exact conditions of Gross's solvent-free procedure. Mass spectrometric analysis of the products suggested the presence of a number of expanded porphyrins, although we did not fully characterize these products in this work. As mentioned in the text, Osuka and co-workers have obtained perfluorinated expanded porphyrins from the condensation of pentafluorobenzaldehyde and 3,4-difluoropyrrole under modified Lindsey conditions. However, while this paper was under review, Chang and co-workers reported that increasing the reaction time and temperature in Gross's solvent-free procedure does allow the successful isolation of perfluorinated *meso*-triphenylcorrole, with pentafluorobenzaldehyde and 3,4-difluoropyrrole as starting materials: Liu, H.-Y.; Lai, T.-S.; Yeung, L.-L.; Chang, C. K. *Org. Lett.* **2003**, *5*, 617−620.
(20) Cai, S.; Walker, F. A.; Licoccia, S. *Inorg. Chem.* **2000**, *39*, 3466.
(21) Zakharieva, O.; Schuenemann, V.; Gerdan, M.; Licoccia, S.; Cai, S.; Walker, F. A.; Trautwein, A. X. *J. Am. Chem. Soc.* **2002**, *124*, 6636.
(22) Cai, S.; Licoccia, S.; D'Ottavi, C.; Paolesse, R.; Nardis, S.; Bulach, V.; Zimmer, B.; Shokhireva, T. K.; Walker, F. A. *Inorg. Chim. Acta* **2002**, *339*, 171.
(23) Walker, F. *Inorg. Chem.* **2003**, *42*, 4526.
(24) Steene, E.; Wondimagegn, T.; Ghosh, A. *J. Phys. Chem. B* **2001**, *105*, 11 406. Addition/Correction: *J. Phys. Chem. B* **2002**, *106*, 5312.
(25) Steene, E.; Wondimagegn, T.; Ghosh, A. *J. Inorg. Biochem.* **2002**, *88*, 113.
(26) Ghosh, A.; Steene, E. *J. Inorg. Biochem.* **2002**, *91*, 423.
(27) Tangen, E.; Ghosh, A. *J. Am. Chem. Soc.* **2002**, *124*, 8117.
(28) Ramdhanie, B.; Stern, C. L.; Goldberg, D. P. *J. Am. Chem. Soc.* **2001**, *123*, 9447.

procedure was that solvent was removed from the final dichloromethane extract of 3,4-difluoropyrrole by blowing a gentle stream of dry $N_2$ over the solution at room temperature for approximately 2 h. Rotary evaporation was avoided to prevent loss of the volatile 3,4-difluoropyrrole.

**General Synthesis of the Free Base β-Octafluoro-*meso*-triarylcorroles.** A 1.5-g portion of basic alumina was placed in an open 50 mL round-bottomed flask with a stirring bar, 3,4-difluoropyrrole (5.92 mmol), an aromatic aldehyde (5.92 mmol), and 1 mL $CH_2Cl_2$. The flask was slowly heated to 70 °C with stirring while the $CH_2Cl_2$ evaporated, and the temperature was then maintained for 4 h. Thereafter, heating was discontinued, 80−100 mL $CH_2Cl_2$ was added, solid residues were dislodged from the walls of the flask with a spatula, the mixture was swirled, and the solids were brought into solution as quickly and as much as possible. DDQ (2.96 mmol) was then added to the solution and the mixture was stirred for an hour. The mixture was then filtered with a Büchner funnel. The filtrate was evaporated to dryness and the dry material was subjected to flash chromatography. The mobile phases used, which varied somewhat for the different corroles synthesized, are indicated below. The corroles eluted were best detected by their UV−visible spectra. All the free-base β-octafluoro-*meso*-triarylcorroles prepared were also found to be strongly fluorescent. Yields: 6−8%.

**Flash Chromatography of β-Octafluoro-*meso*-tris(*p*-trifluoromethylphenyl)corrole, $H_3[F_8T(p\text{-}CF_3\text{-}P)C]$.** The crude corrole was first passed through a short column (∼10 cm) of silica gel with $CH_2Cl_2$ as eluent. The product from this column was then passed through a longer column (∼22 cm) of silica gel with *n*-hexane/$CH_2Cl_2$, 3:1 initially and then 2:1, as eluents.

**Flash Chromatography of β-Octafluoro-*meso*-triphenylcorrole, $H_3[F_8TPC]$.** The crude corrole was first passed through a short column (∼10 cm) of silica gel with $CH_2Cl_2$ and then 3% MeOH in $CH_2Cl_2$ as eluents. The product from this column was then passed through a longer column (∼22 cm) of silica gel with *n*-hexane/$CH_2Cl_2$, 3:1 initially and then 2:1, as eluents.

**Flash Chromatography of β-Octafluoro-*meso*-tris(*p*-methylphenyl)corrole, $H_3[F_8T(p\text{-}CH_3\text{-}P)C]$.** The crude corrole was first passed through a short column (∼10 cm) of silica with $CH_2Cl_2$ and then 3% MeOH in $CH_2Cl_2$ as eluents. The product from this column was then passed through a longer column (∼22 cm) of silica gel with *n*-hexane/$CH_2Cl_2$, 3:1initially and then 2.5:1, as eluents.

**Flash Chromatography of β-Octafluoro-*meso*-tris(*p*-methoxyphenyl)corrole, $H_3[F_8T(p\text{-}OCH_3\text{-}P)C]$.** The crude corrole was first passed through a short column (∼10 cm) of silica gel with $CH_2Cl_2$ as eluent. The product from this column was then passed through a longer column (∼22 cm) of silica gel with successively 1:1, 1:2, and 1:3 *n*-hexane/$CH_2Cl_2$ as eluents.

**General Synthesis of Cu β-Octafluoro-*meso*-triarylcorroles.** Free-base β-octafluoro-*meso*-triarylcorrole (∼0.040 g) was dissolved in 25 mL pyridine at room temperature, five equivalents of $Cu(OAc)_2{\cdot}4H_2O$ were added, and the mixture was stirred for 15 min. The pyridine was removed by rotary evaporation and the pure product was obtained by flash chromatography of the residue on silica gel using 2:1 *n*-hexane/$CH_2Cl_2$ as eluent. Yields: 85−98%.

**General Synthesis of FeCl β-Octafluoro-*meso*-triarylcorroles.** Free-base β-octafluoro-*meso*-triarylcorrole (∼0.040 g) was dissolved in 25 mL methanol and heated to reflux. Five equivalents of $FeCl_2{\cdot}4H_2O$ were added, and the reaction was monitored by UV−visible spectroscopy. After the solution had been heated for 5−30 min and no more changes occurred in the UV−visible spectra, heating was discontinued. The methanol was removed by rotary evaporation and the product was dissolved in $CH_2Cl_2$ and extracted three times with 2 M aqueous HCl. The solvent was again removed by rotary evaporation and the crude product was chromatographed on silica gel using $CH_2Cl_2$ and then 2% MeOH in $CH_2Cl_2$ as eluent. On the basis of NMR analysis, the product form the column appeared to be the iron chloride and small amounts of the iron μ-oxo dimer corrole complex. We obtained the pure iron chloride by extracting a solution of the crude product in $CH_2Cl_2$, i.e., the eluate from the column chromatography, three times with 2 M HCl and then removing the $CH_2Cl_2$ by rotary evaporation. Bubbling of HCl gas through a solution of the crude product can be used as an alternative to extraction for all the analogues except for the *p*-$CF_3$ analogue for which this treatment seems to result in demetalation of the macrocycle. Yields: 55−85%.

**Characterization.** The compounds were characterized by electronic absorption, $^1$H NMR, and $^{19}$F NMR spectroscopies, MALDI-TOF mass spectrometry, and elemental analysis. Elemental analyses of all but two of the compounds, viz. Cu[$F_8$T(*p*-$CF_3$−P)C] and Cu[$F_8$T(*p*-$CH_3$−P)C], were within 0.5% of the theoretical values. However, even the two recalcitrant compounds were judged to be pure on the basis of their $^1$H NMR, $^{19}$F NMR, and MALDI-TOF mass spectra, as indicated below. The following describes the characterization of the new compounds reported here. The $^1$H and $^{19}$F NMR spectra are also included as Supporting Information.

**$H_3[F_8T(p\text{-}CF_3\text{-}P)C]$.** UV−vis: $\lambda_{max}$ (log $\epsilon$/($M^{-1}$ $cm^{-1}$)) 404 nm (5.09), 503 nm (3.91) 540 nm (4.13), 632 nm (4.00). $^1$H NMR (in the presence of a small drop of $CF_3COOH$): $\delta$ 8.28 (d, $J$ = 8.0 Hz, 4H, 5,15-*o*- or *m*-phenyl), 8.19 (d, $J$ = 8.0 Hz, 2H 10-*o*- or *m*-phenyl), 8.00 (d, $J$ = 8.0 Hz, 4H, 5,15-*o*- or *m*-phenyl), 7.95 (d, $J$ = 8.0 Hz, 2H, 10-*o*- or *m*-phenyl). $^{19}$F NMR (in the presence of a small drop of $CF_3COOH$): $\delta$ −62.12 (s, 3F, 10-*p*-$CF_3$), −62.19 (s, 6F, 5,15-*p*-$CF_3$), −147.1 (s, 2F, β-pyrrolic), −148.1 (s, 2F, β-pyrrolic), −148.8 (s, 2F, β-pyrrolic), −158.8 (s, 2F, β-pyrrolic). MS (MALDI-TOF, major isotopomer): $M^+$ = 873.96 (expt.), 874.10 (calcd.). Elemental analysis: 54.75%C (calcd. 54.93%), 1.92%H (calcd. 1.73%), 6.29%N (calcd. 6.41%).

**$H_3[F_8TPC]$.** UV−vis: $\lambda_{max}$ (log $\epsilon$/($M^{-1}$ $cm^{-1}$)) 403 nm (4.99), 495 nm (3.99), 537 nm (4.02), 633 nm (4.00). $^1$H NMR (in the presence of a small drop of $CF_3COOH$): 7.69−7.33 (m, 15H, all phenyl protons). $^{19}$F NMR (in the presence of a small drop of $CF_3COOH$): $\delta$ −145.3 (s, 2F, β-pyrrolic), −148.1 (s, 2F, β-pyrrolic), −149.1 (s, 2F, β-pyrrolic), −155.6 (s, 2F, β-pyrrolic). MS (MALDI-TOF, major isotopomer): $M^+$ = 670.02 (expt.), 670.14 (calcd.). Elemental analysis: 66.03%C (calcd. 66.27%), 2.91%H (calcd. 2.71%), 8.23%N (calcd. 8.36%).

**$H_3[F_8T(p\text{-}CH_3\text{-}P)C]$.** UV−vis: $\lambda_{max}$ (log $\epsilon$/($M^{-1}$ $cm^{-1}$)) 405 nm (5.03), 503 nm (3.94), 540 nm (4.10), 637 nm (4.09). $^1$H NMR (in the presence of a small drop of $CF_3COOH$): $\delta$ 7.10−7.70 (m, 12H, all phenyl protons), 2.65 (s, 9H, 5,10,15-*p*-$CH_3$). $^{19}$F NMR (in the presence of a small drop of $CF_3COOH$): $\delta$ -145.7 (s, 2F, β-pyrrolic), −148.4 (s, 2F, β-pyrrolic), −149.5 (s, 2F, β-pyrrolic), −155.8 (s, 2F, β-pyrrolic). MS (MALDI-TOF, major isotopomer): $M^+$ = 712.26 (expt.), 712.19 (calcd.). Elemental analysis: 67.60%C (calcd. 67.42%), 3.57%H (calcd. 3.39%), 7.80%N (calcd. 7.86%).

**$H_3[F_8T(p\text{-}OCH_3\text{-}P)C]$.** UV−vis: $\lambda_{max}$ (log $\epsilon$/($M^{-1}$ $cm^{-1}$)) 410 nm (5.13), 505 nm (3.98), 544 nm (4.18), 642 nm (4.23). $^1$H NMR (in the presence of a small drop of $CF_3COOH$): $\delta$ 8.12 (s, 4H, 5,15-*o*- or *m*-phenyl), 8.05 (s, 2H, 10-*o*- or *m*-phenyl), 7.32 (d, 6H, 5,15-*o*- or *m*-phenyl and 10-*o*- or *m*-phenyl), 4.05 (s, 9H, 5,10,15-*p*-$OCH_3$). $^{19}$F NMR (in the presence of a small drop of $CF_3COOH$): $\delta$ −148.2 (s, 2F, β-pyrrolic), −150.8 (s, 2F, β-pyrrolic), −152.5 (s, 2F, β-pyrrolic), −159.0 (s, 2F, β-pyrrolic). MS (MALDI-TOF, major isotopomer): $M^+$ = 760.35 (expt.), 760.17 (calcd.). Elemental analysis: 62.99%C (calcd. 63.16%), 3.30%H (calcd. 3.18%), 7.19%N (calcd. 7.37%).

**Cu$[F_8T(p\text{-}CF_3\text{-}P)C]$.** UV−vis: $\lambda_{max}$ (log $\epsilon$/($M^{-1}cm^{-1}$)) 401 nm (4.92). $^1$H NMR: $\delta$ 7.69 (d, $J$ = 8.0 Hz, 4H, 5,15-*o*- or *m*-phenyl), 7.64 (d, $J$ = 8.0 Hz, 2H 10-*o*- or *m*-phenyl), 7.57 (d, $J$ = 8.0 Hz, 4H, 5,15-*o*- or *m*-phenyl), 7.40 (d, $J$ = 8.0 Hz, 2H, 10-*o*- or *m*-phenyl). $^{19}$F NMR: $\delta$ −63.27 (s, 6F, 5,15-*p*-$CF_3$), −63.30 (s, 3F, 10-*p*-$CF_3$), −143.9 (s, 2F, β-pyrrolic), −145.5 (s, 2F, β-pyrrolic), −146.5 (s, 2F, β-pyrrolic),

(29) Woller, E. K.; Smirnov, V. V.; DiMagno, S. G. *J. Org. Chem.* **1998**, *63*, 5706.

−152.9 (s, 2F, β-pyrrolic). MS (MALDI-TOF, major isotopomer): $M^+$ = 934.10 (expt.), 934.01 (calcd.).

**Cu[$F_8$TPC].** UV−vis: $\lambda_{max}$ (log $\epsilon$/($M^{-1}$ $cm^{-1}$)) 409 nm (4.91). $^1$H NMR: δ 7.57 (t, $J$ = 6.8 Hz, 2H, 10-*m*-phenyl or 5,15-*p*-phenyl), 7.50 (d, $J$ = 6.0 Hz, 4H 5,15-*o*-phenyl), 7.44−7.34 (m, 7H, 5,15-*m*-phenyl, 10-*p*-phenyl and 5,15-*p*-phenyl or 10-*o*- or *m*-phenyl), 7.24 (s, 2H, 5,15-*p*-phenyl or 10-*o*- or *m*-phenyl; overlaps with $CHCl_3$ peak). $^{19}$F NMR: δ −144.9 (s, 2F, β-pyrrolic), −146.7 (s, 2F, β-pyrrolic), −147.7 (s, 2F, β-pyrrolic), −154.7 (s, 2F, β-pyrrolic). MS (MALDI-TOF, major isotopomer): $M^+$ = 730.23 (expt.), 730.05 (calcd.). Elemental analysis: 60.95%C (calcd. 60.79%), 2.19%H (calcd. 2.07%), 7.48%N (calcd. 7.66%).

**Cu[$F_8$T(*p*-$CH_3$-P)C].** UV−vis: $\lambda_{max}$ (log $\epsilon$/($M^{-1}$ $cm^{-1}$)) 380 nm (4.73, sh.), 421 nm (4.97). $^1$H NMR: δ 7.40 (d, $J$ = 7.6 Hz, 4H, 5,15-*o*- or *m*-phenyl), 7.24 (d, 2H, 10-*o*- or *m*-phenyl; overlaps with $CHCl_3$ peak), 7.20 (d, $J$ = 7.6 Hz, 4H, 5,15-*o*- or *m*-phenyl), 7.14 (d, $J$ = 7.2 Hz, 2H, 10-*o*- or *m*-phenyl), 2.38 (s, 6H, 5,15-*p*-$CH_3$), 2.34 (s, 3H, 10-*p*-$CH_3$). $^{19}$F NMR: δ -145.2 (s, 2F, β-pyrrolic), −147.2 (s, 2F, β-pyrrolic), −148.2 (s, 2F, β-pyrrolic), −155.3 (s, 2F, β-pyrrolic). MS (MALDI-TOF, major isotopomer): $M^+$ = 771.99 (expt.), 772.09 (calcd.).

**Cu[$F_8$T(*p*-$OCH_3$-P)C].** UV−vis: $\lambda_{max}$ (log $\epsilon$/($M^{-1}$ $cm^{-1}$)) 380 nm (4.78), 436 nm (4.85), 535 nm (4.24, broad). $^1$H NMR: δ 7.53 (d, $J$ = 8.0 Hz, 4H, 5,15-*o*- or *m*-phenyl), 7.40 (d, $J$ = 8.4 Hz, 2H, 10-*o*- or *m*-phenyl), 6.93 (d, $J$ = 8.0 Hz, 4H, 5,15-*o*- or *m*-phenyl), 6.88 (d, $J$ = 8.0 Hz, 2H, 10-*o*- or *m*-phenyl), 3.88 (s, 6H, 5,15-*p*-$OCH_3$), 3.86 (s, 3H, 10-*p*-$OCH_3$). $^{19}$F NMR: δ −145.5 (s, 2F, β-pyrrolic), −147.6 (s, 2F, β-pyrrolic), −148.9 (s, 2F, β-pyrrolic), −155.8 (s, 2F, β-pyrrolic). MS (MALDI-TOF, major isotopomer): $M^+$ = 820.11 (expt.), 820.08 (calcd.). Elemental analysis: 58.26%C (calcd. 58.51%), 2.78%H (calcd. 2.58%), 6.66%N (calcd. 6.82%).

**Fe[$F_8$T(*p*-$CF_3$-P)C]Cl.** UV−vis: $\lambda_{max}$ (log $\epsilon$/($M^{-1}cm^{-1}$)) 353 nm (4.78). $^1$H NMR: δ 19.9 (s, 2H, 5,15-*o*-phenyl), 19.0 (s, 2H, 5,15-*o*-phenyl), 18.0 (s, 2H, 10-*o*-phenyl), −1.16 (s, 2H, 5,15-*m*-phenyl), −1.42 (s, 2H, 5,15-*m*-phenyl), −2.14 (s, 2H, 10-*m*-phenyl). $^{19}$F NMR: δ -32.2 (s, 2F, β-pyrrolic), −40.5 (s, 2F, β-pyrrolic), −47.0 (s, 2F, β-pyrrolic), −59.9 (s, 2F, β-pyrrolic), −69.2 (s, 3F, 10-*p*-$CF_3$), −71.5 (s, 6F, 5,15-*p*-$CF_3$). MS (MALDI-TOF, major isotopomer): $M^+$ − Cl = 927.25 (expt.), 927.01 (calcd.). Elemental analysis: 50.14%C (calcd. 49.90%), 1.46%H (calcd. 1.26%), 5.96%N (calcd. 5.82%).

**Fe[$F_8$TPC]Cl.** UV−vis: $\lambda_{max}$ (log $\epsilon$/($M^{-1}$ $cm^{-1}$)) 355 nm (4.73). $^1$H NMR: δ 20.9 (s, 2H, 5,15-*o*-phenyl), 20.1 (s, 2H, 5,15-*o*-phenyl), 18.8 (s, 2H, 10-*o*-phenyl), 15.5 (s, 2H, 5,15-*p*-phenyl), 13.0 (s, 1H, 10-*p*-phenyl), −2.16 (s, 2H, 5,15-*m*-phenyl), −2.39 (s, 2H, 5,15-*m*-phenyl), −3.29 (s, 2H, 10-*m*-phenyl). $^{19}$F NMR: δ −29.8 (s, 2F, β-pyrrolic), −44.3 (s, 2F, β-pyrrolic), −52.9 (s, 2F, β-pyrrolic), −58.3 (s, 2F, β-pyrrolic). MS (MALDI-TOF, major isotopomer): $M^+$ − Cl = 723.51 (expt.), 723.05 (calcd.). Elemental analysis: 58.74%C (calcd. 58.56%), 2.19%H (calcd. 1.99%), 7.19%N (calcd. 7.38%).

**Fe[$F_8$T(*p*-$CH_3$-P)C]Cl.** UV−vis: $\lambda_{max}$ (log $\epsilon$/($M^{-1}$ $cm^{-1}$)) 360 nm (4.78). $^1$H NMR: δ 22.0 (s, 2H, 5,15-*o*-phenyl), 21.2 (s, 2H, 5,15-*o*-phenyl), 19.7 (s, 2H, 10-*o*-phenyl), −2.98 (s, 2H, 5,15-*m*-phenyl), −3.16 (s, 2H, 5,15-*m*-phenyl), −4.25 (s, 2H, 10-*m*-phenyl), −5.08 (s, 3H, 10-*p*-$CH_3$), −8.12 (s, 6H, 5,15-*p*-$CH_3$). $^{19}$F NMR: δ −29.6 (s, 2F, β-pyrrolic), −46.8 (s, 2F, β-pyrrolic), −55.5 (s, 2F, β-pyrrolic), −57.4 (s, 2F, β-pyrrolic). MS (MALDI-TOF, major isotopomer): $M^+$ − Cl = 765.54 (expt.), 765.10 (calcd.). Elemental analysis: 59.96%C (calcd. 59.99%), 2.90%H (calcd. 2.64%), 6.76%N (calcd. 7.00%).

**Fe[$F_8$T(*p*-$OCH_3$-P)C]Cl.** UV−vis: $\lambda_{max}$ (log $\epsilon$/($M^{-1}cm^{-1}$)) 367 nm (4.80). $^1$H NMR: δ 23.2 (s, 2H, 5,15-*o*-phenyl), 22.7 (s, 2H, 5,15-*o*-phenyl), 20.9 (s, 1H, 10-*o*-phenyl), 20.7 (s, 1H, 10-*o*-phenyl), −2.09 (s, 4H, 5,15-*m*-phenyl), −3.36 (s, 1H, 10-*m*-phenyl), −3.41 (s, 1H, 10-*m*-phenyl), 2.34 (s, 3H, 10-*p*-$OCH_3$), 1.86 (s, 6H, 5,15-*p*-$OCH_3$). $^{19}$F NMR: δ −27.8 (s, 2F, β-pyrrolic), −50.3 (s, 2F, β-pyrrolic), −57.7 (s, 4F, β-pyrrolic; two overlapping peaks). MS (MALDI-TOF, major isotopomer): $M^+$ − Cl = 813.17 (expt.), 813.08 (calcd.). Elemental analysis: 56.55%C (calcd. 56.59%), 2.64%H (calcd. 2.49%), 6.41%N (calcd. 6.60%).

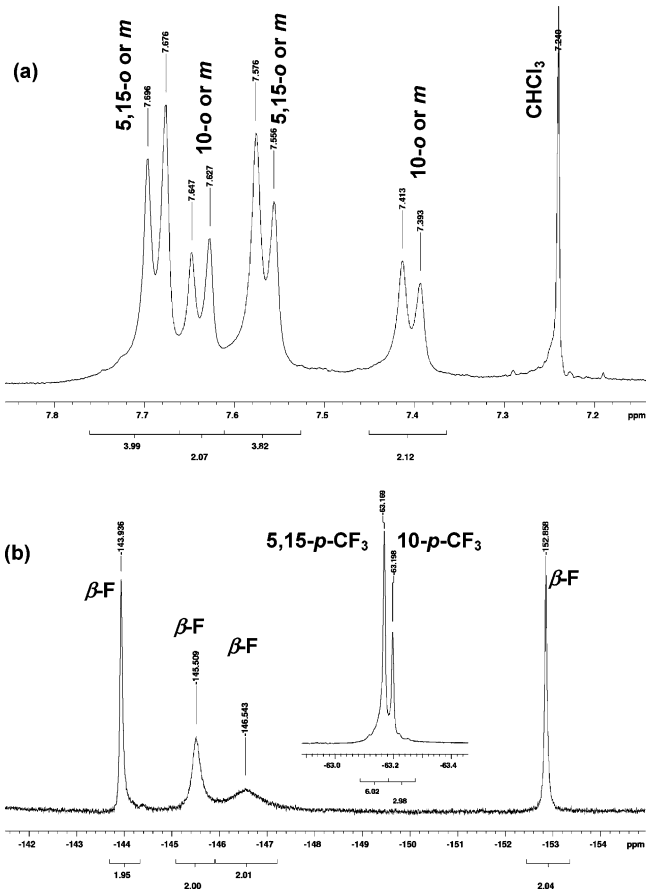


***Figure 2.*** (a) $^1$H and (b) $^{19}$F NMR spectra of Cu[$F_8$T(*p*-$CF_3$−P)C].

**DFT Calculations**. DFT calculations on FeCl corrole and β-octafluorocorrole were carried out using Slater-type valence triple-ζ plus polarization basis sets, the VWN local functional, the Perdew−Wang 1991 gradient corrections, a spin-unrestricted formalism, a fine mesh for numerical integration of matrix elements, full geometry optimizations with $C_s$ symmetry constraints, and the ADF [30] program system. Similar calculations with $C_{2v}$ symmetry constraints and full geometry optimizations were also carried out for three electronic states of copper octafluorocorrole: (a) the S = 0 Cu(III) state, (b) a $^3A_2$ Cu(II) corrole $b_1$ radical state, and (c) a $^3B_1$ Cu(II) corrole $a_2$ radical state.

## Results and Discussion

**NMR Spectroscopy.** Figure 2 shows the room-temperature $^1$H and $^{19}$F NMR spectra of Cu[$F_8$T(*p*-$CF_3$−P)C]. The $^1$H NMR spectrum exhibits four doublets (ratio = 2:2:1:1, total of 12 protons) in the aromatic region which correspond to the *ortho*- and *meta*-protons of the symmetry-equivalent 5- and 15-aryl groups (two doublets of 4 protons each) and of the 10-aryl group (two doublets of 2 protons each). The $^{19}$F NMR spectrum exhibits two peaks around −63 ppm (ratio = 2:1, total of 9 fluorines) corresponding to the *para*-$CF_3$ groups on the symmetry-equivalent 5- and 15-aryl groups and on the 10-aryl group, respectively. Four peaks also occur in the −143 to −153 ppm (ratio = 1:1:1:1, total 8 fluorines) range corresponding to the

(30) The ADF program system was obtained from Scientific Computing and Modeling, Department of Theoretical Chemistry, Vrije Universiteit, 1081 HV Amsterdam, The Netherlands. For details of basis sets, grids for numerical integration, etc., the reader is referred to the program manual obtainable from this source.

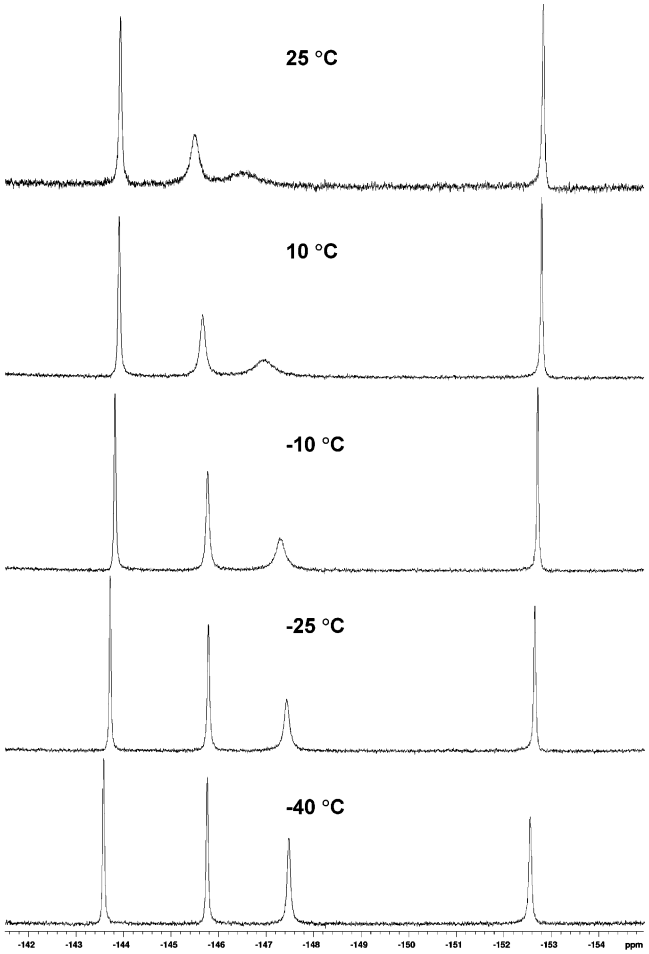


***Figure 3.*** $^{19}$F NMR spectra of Cu[$F_8$T(*p*-$CF_3$−P)C] at various temperatures.

$\beta$-fluorines, two of which are seen to couple in the $^{19}$F−$^{19}$F COSY spectrum (see Supporting Information Figure S28). As might be expected, the $^1$H and $^{19}$F NMR spectra of Cu[$F_8$TPC], Cu[$F_8$T(*p*-$CH_3$−P)C], and Cu[$F_8$T(*p*-$OCH_3$−P)C] (see Supporting Information Figures S15−S27) are qualitatively similar to those of Cu[$F_8$T(*p*-$CF_3$−P)C].

The $^1$H and $^{19}$F NMR spectra of the Cu corroles are qualitatively very similar to those of the protonated free-base corroles (see Supporting Information Figures S36−S45).[31] Not a great deal of comment is warranted on the latter spectra except for a couple of points. Thus, neither the free bases nor the Cu complexes exhibit $^{19}$F peaks that are doublets, which implies very small $^{19}$F−$^{19}$F *J*-couplings in both classes of compounds. This is consistent with the small *J*-couplings (3−5 Hz) observed for the $\beta$-protons of the Cu derivatives of $\beta$-unfluorinated triarylcorroles.[17]

The $^{19}$F NMR spectra of the Cu octafluorocorroles exhibit a remarkable temperature dependence: for each Cu complex, two of the four $\beta$-$^{19}$F peaks broaden significantly with temperature between −40 and +40 °C, as shown for Cu[$F_8$T(*p*-$CF_3$−P)C] in Figure 3, which is quite unlike the behavior of the protonated free bases. The temperature-dependent $^{19}$F NMR behavior of the Cu octafluorocorroles is reminiscent of similar behavior observed in the $^1$H NMR spectra of a copper $\beta$-octaalkylcorrole by E. Vogel, M. Gross and co-workers,[32] who attributed their observation to a thermally accessible copper(II) corrole $\pi$-cation radical excited state. We suggest that a similar scenario holds for the copper octafluorocorroles reported here. The fact that only two of the four $\beta$-$^{19}$F peaks broaden significantly with temperature may reflect the fact that only two of the four symmetry-unique $\beta$-positions of a corrole $b_1$-type radical carry significant spin density.[33] We also investigated the electronic absorption and Soret-resonant Raman spectra[34] of the Cu octafluorocorroles as a function of temperature, but these remained essentially unchanged at low temperatures, suggesting that the diamagnetic Cu(III) ground state is the dominant species between −40 °C and 40 °C.

Figure 4 shows the room-temperature $^1$H and $^{19}$F NMR spectra of Fe[$F_8$TPC]Cl. The other three FeCl complexes, viz. Fe[$F_8$T(*p*-$CF_3$−P)C]Cl, Fe[$F_8$T(*p*-$CH_3$−P)C]Cl, and Fe[$F_8$T(*p*-$OCH_3$−P)C]Cl, exhibit similar spectra (see Supporting Information Figures S3−S15). The general pattern of peaks observed in the $^1$H NMR spectra of these complexes is similar to what has previously been observed for their $\beta$-unsubstituted analogues[22,24] except that the $\beta$-proton peaks obviously are missing for the present compounds. All peaks in the $^1$H NMR spectra were assigned based on COSY experiments (see Figures S4, S8, S11, and S14 in the Supporting Information). Note that the *ortho* (as well as the *meta*) protons of the 10-aryl group in all these complexes should have given rise to two peaks in the spectra, as is the case for the *ortho* and *meta* protons of the symmetry-equivalent 5- and 15-aryl groups. However, for the 10-aryl group, only one peak for the *ortho* protons and one for the *meta* protons are observed for the *p*-$CF_3$, *p*-H, and *p*-$CH_3$ FeCl derivatives, because these peaks are not resolved at 400 MHz. In contrast, for the *p*-$OCH_3$ FeCl derivative, the peaks are only partially overlapping and there are two peaks both for the *ortho* and for the *meta* protons of the 10-aryl group. Similar overlapping peaks for the two symmetry-distinct *ortho* and *meta* protons in the 10-aryl group are also observed for the FeCl complexes of $\beta$-unfluorinated *meso*-triarylcorroles.[22,24]

Table 1 summarizes the isotropic shifts ($\delta_{iso}$) of all $^1$H and $^{19}$F peaks as well as their assignments for the four FeCl $\beta$-octafluoro-*meso*-triarylcorroles reported in this paper, along with analogous data for some other relevant FeCl *meso*-triarylcorroles. The substantial isotropic shifts seen for the phenyl protons of the $\beta$-fluorinated complexes are qualitatively similar to those seen for their $\beta$-unsubstituted analogues,[22,24]

(31) The line widths of the $^1$H and $^{19}$F NMR peaks of the protonated free-base corroles are sensitive to the amount of acid present in the NMR samples. We have not investigated this phenomenon in depth but have empirically found that the sharpest spectra are obtained with only a small drop of added trifluoroacetic acid. Excess acid leads to peak broadening in these spectra.

(32) Will, S.; Lex, J.; Vogel, E.; Schmickler, H.; Gisselbrecht, J.-P.; Haubtmann, C.; Bernard, M.; Gross, M. *Angew. Chem., Int. Ed. Engl.* **1997**, *36*, 357. For a new, relevant article, see: Bruckner, C.; Brinas, R. P.; Krause Bauer, J. A. *Inorg. Chem.* **2003**, *42*, 4495.

(33) Ghosh, A.; Wondimagegn, T.; Parusel, A. B. J. *J. Am. Chem. Soc.* **2000**, *122*, 5100.

(34) These Resonance Raman (RR) spectra can be found in Figures S32−S35 of the Supporting Information. Because these spectra have not been assigned, we refrain from describing them in detail. We only note, however, that an intense high-frequency marker band at approximately 1487−1492 $cm^{-1}$ for the $\beta$-unsubstituted copper triarylcorroles[17] appears to downshift to 1461−1467 $cm^{-1}$ for the Cu $\beta$-octafluorocorroles studied here and to 1458−1462 $cm^{-1}$ for Cu $\beta$-octabromocorroles.[17] We speculate that this vibration has C$\beta$−C$\beta$ stretching character which would indicate that $\beta$-octafluorination and $\beta$-octabromination have a comparable bond-lengthening influence on the C$\beta$−C$\beta$ bonds. Because $\beta$-octafluorination and $\beta$-octabromination may be expected to induce different degrees of nonplanarity on the corrole ring, the similarity of this frequency for the two classes of halogenated copper corroles may indicate that the halogenation-induced downshift of this vibration reflects a direct bond-lengthening effect of the $\beta$-halogen substituents on the C$\beta$−C$\beta$ bonds rather than a nonplanarity effect.

***Table 1.*** $^1$H and $^{19}$F NMR Isotropic Shifts[a] (ppm) for Different FeCl *Meso*-triarylcorroles

| | | isotropic shifts (ppm)[a] | | | | | | | | |
|---|---|---|---|---|---|---|---|---|---|---|
| compound | conditions | 5,15-*o*-H | 10-*o*-H | 5,15-*m*-H | 10-*m*-H | 5,15-*p*-H | 10-*p*-H | 5,15-*p*-$CF_3$/ $CH_3$/$OCH_3$ | 10-*p*-$CF_3$/ $CH_3$/$OCH_3$ | β-pyrrole H/F |
| Fe[$F_8$T(*p*-$CF_3$-P)C]Cl[b] | $CDCl_3$, 298 K | 12.2(2H), 11.4(2H) | 10.3(2H) | −8.64(2H), −8.88(2H) | −9.61(2H) | | | −8.25(6F) | −5.88(3F) | 115(2F), 107(2F), 100(2F), 87.3(2F) |
| Fe[$F_8$TPC]Cl[b] | $CDCl_3$, 298 K | 13.4(2H), 12.6(2H) | 11.3(2H) | −9.67(2H), −9.90(2H) | −10.8(2H) | 7.98(2H) | 5.46(1H) | | | 119(2F), 104(2F), 95.6(2F), 90.2(2F) |
| Fe[$F_8$T(*p*-$CH_3$-P)C]Cl[b] | $CDCl_3$, 298 K | 14.6(2H), 13.8(2H) | 12.3(2H) | −10.3(2H), −10.4(2H) | −11.5(2H) | | | −10.5(6H) | −7.44(3H) | 119(2F), 102(2F), 93.4(2F), 91.4(2F) |
| Fe[$F_8$T(*p*-$OCH_3$-P)C]Cl[b] | $CDCl_3$, 298 K | 16.0(2H), 15.5(2H) | 13.7(1H), 13.5(1H) | −9.29(4H) | −10.6(1H), −10.6(1H) | | | −2.02(6H) | −1.52(3H) | 122(2F), 99.2(2F), 91.8(4F) |
| Fe[T(*p*-$CF_3$-P)C]Cl[24] | $CDCl_3$, rt | 16.3(2H), 15.1(2H) | 14.3(2H) | −9.45(2H), −9.65(2H) | −10.5(1H), −10.6(1H) | | | | | −2.15(2H), −14.0(2H), −14.5(2H), −47.5(2H) |
| Fe[TPC]Cl[24] | $CDCl_3$, rt | 17.6(2H), 16.4(2H) | 15.5(2H) | −10.2(2H), −10.5(2H) | −11.3(1H), −11.5(1H) | 12.0(2H) | 9.68(1H) | | | −1.59(2H), −13.4(2H), −14.5(2H), −48.7(2H) |
| Fe[T(*p*-$CH_3$-P)C]Cl[24] | $CDCl_3$, rt | 18.5(2H), 17.2(2H) | 16.4(2H) | −10.8(2H), −11.0(2H) | −12.0(1H), −12.4(1H) | | | −14.3(6H) | −12.0(3H) | −1.85(2H), −12.9(2H), −14.8(2H), −48.9(2H) |
| Fe[T(*p*-$OCH_3$-P)C]Cl[22] | $CD_2Cl_2$, 293 K | 18.9(2H), 17.7(2H) | 17.0(1H), 16.8(1H) | −11.3(2H), −11.5(2H) | −12.6(1H), −13.0(1H) | | | | | −1.9(2H), −12.6(2H), −21.5(2H), −45.3(2H) |
| Fe[T(*p*-$NO_2$-P)C]Cl[22] | $CD_2Cl_2$, 303 K | 14.6(2H), 13.6(2H) | 12.8(2H) | −9.5(2H), −9.8(2H) | −10.5(1H), −10.6(1H) | | | | | −2.2(2H), −14.2(2H), −15.4(2H), −46.1(2H) |

[a] The isotropic shifts were calculated by subtracting the corresponding diamagnetic shifts from the chemical shifts. Average $^1$H diamagnetic shifts of 7.7 ppm for Cu[T(*p*-$CF_3$−P)C], 7.6 ppm for Cu[TPC], 7.5 ppm for Cu[T(*p*-$CH_3$−P)C], 7.6 ppm for Cu[$F_8$T(*p*-$CF_3$−P)C], 7.5 ppm for Cu[$F_8$TPC], 7.3 ppm for Cu[$F_8$T(*p*-$CH_3$−P)C], and 7.2 ppm for Cu[$F_8$T(*p*-$OCH_3$−P)C] were used for the pyrrole and phenyl $^1$H peaks because not all these peaks have been assigned for neither the copper complexes, nor the iron complexes. For the same reason, average $^{19}$F diamagnetic shifts of −147.2 ppm for Cu[$F_8$T(*p*-$CF_3$−P)C], −148.5 ppm for Cu[$F_8$TPC], −149.0 ppm for Cu[$F_8$T(*p*-$CH_3$−P)C], and −149.5 ppm for Cu[$F_8$T(*p*-$OCH_3$−P)C] were used for the pyrrole $^{19}$F peaks. [b] This work.

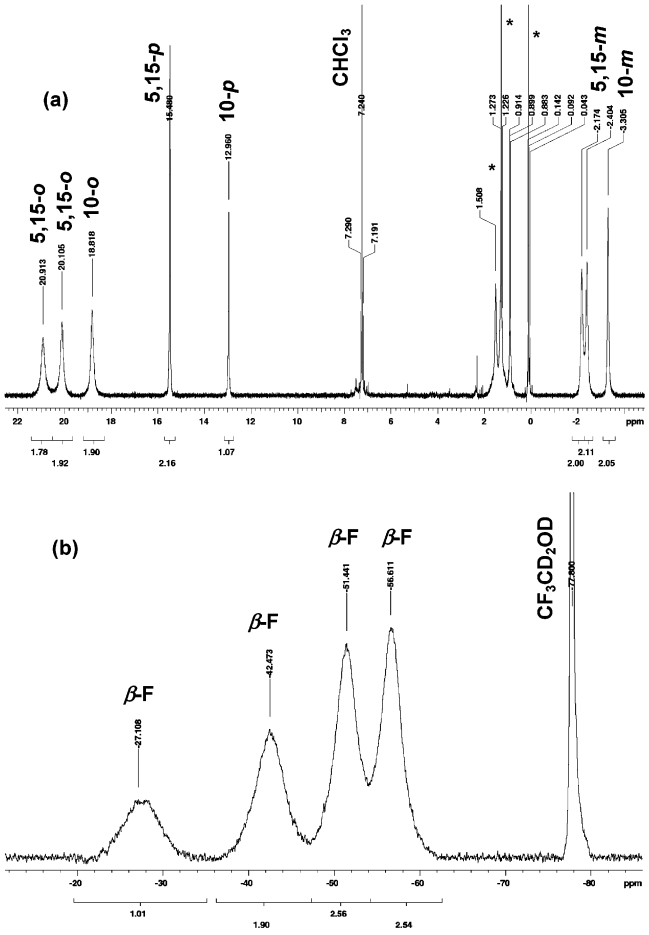


***Figure 4.*** (a) $^1$H and (b) $^{19}$F NMR spectra of Fe[$F_8$TPC]Cl.

indicating the presence of substantial radical character at the *meso* positions. As noted by Walker and co-workers for a number of other FeCl triarylcorroles,[22,23] the isotropic shifts of the *meso*-phenyl protons alternate in sign around the phenyl ring (e.g., *p*-H and *o*-H positive, *m*-H negative) in the new octafluorinated complexes. These signs are opposite to the ones in Fe[(TPP)(*t*-BuNC)$_2$]$^+$, which have been shown to have large positive $\pi$ spin density on the *meso* carbons.[35,36] Hence, in FeCl β-octafluoro-*meso*-triarylcorroles, as well as in their β-unsubstituted analogues, there is substantial negative $\pi$ spin density on the *meso* positions of the corrole ligand, which in turn indicates antiferromagnetic coupling between a corrolate $\pi$-cation radical and an $S = 3/2$ iron center. Table 1 also shows that the isotropic shifts for the FeCl β-octafluoro-*meso*-triarylcorroles are somewhat smaller than for the corresponding β-unsubstituted analogues, indicating somewhat less radical character on the corrole macrocycle. The electron-deficient fluorinated corroles are thus somewhat less noninnocent than "ordinary" corroles.

Gratifyingly, the FeCl octafluorocorroles also yielded broad but distinctly discernible $^{19}$F NMR signals (Figure 4b). Until now, the only significant $^{19}$F NMR study of relevant paramagnetic compounds is one by Yatsunyk and Walker[37] on iron(III) *meso*-pentafluorophenyl porphyrins and corroles, but this study necessarily focused on only phenyl-bound fluorines. We were therefore intrigued by the possibility that the present FeCl corroles, being β-fluorinated, might exhibit very large $^{19}$F isotropic shifts and thereby advance our understanding of $^{19}$F NMR chemical shifts in paramagnetic compounds in general. Although a complete treatment of this topic is outside the scope of this paper, a few interesting observations pertaining to this issue may be made. If we choose the mean of the chemical shifts of the β-fluorines in the copper complexes as the reference (for calculating the isotropic shifts), then the isotropic shifts of the β-fluorines in the corresponding FeCl complexes span a range of 87−122 ppm, as shown in Table 1. While signifi-

(35) Simonneaux, G.; Hindre, F.; Le Plouzennec, M. *Inorg. Chem.* **1989**, *28*, 823.
(36) Walker, F. A. In *The Porhyrin Handbook*; Kadish, K. M., Smith, K. M., Guilard, R., Eds.; Academic Press: San Diego, 2000; Vol. 5, p 81.
(37) Yatsunyk, L.; Walker, F. A. *Inorg. Chim. Acta* **2002**, *337*, 266.

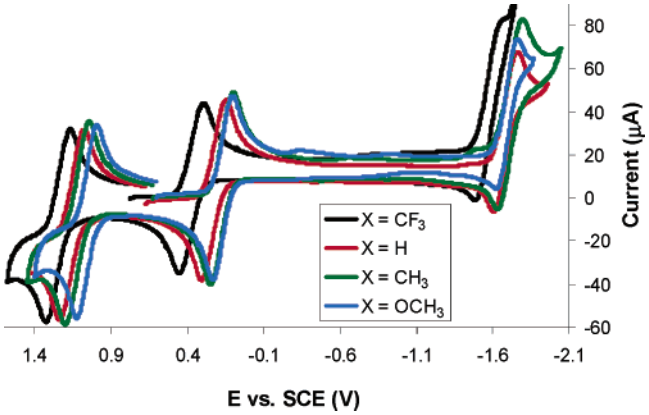


***Figure 5.*** Cyclic voltammograms of the Cu $\beta$-octafluoro-*meso*-tris(*p*-X-phenyl)corroles (X = $OCH_3$, $CH_3$, H, and $CF_3$) prepared in this work.

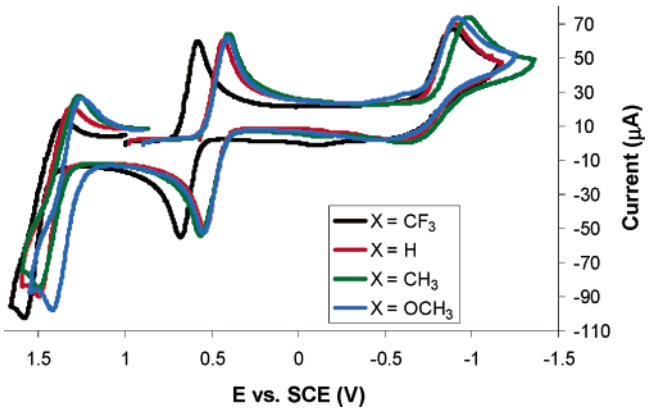


***Figure 6.*** Cyclic voltammograms of the FeCl $\beta$-octafluoro-*meso*-tris(*p*-X-phenyl)corroles (X = $OCH_3$, $CH_3$, H, and $CF_3$) prepared in this work.

cant and indeed larger than those observed for Fe(TPFPC)Cl (TPFPC = *meso*-tris(pentafluoropenyl)corrole),[22] these shifts are by no means enormous, indicating that the highly electronegative fluorine atoms carry only relatively modest spin densities, i.e., relatively little of the $\pi$-cation radical character of the corrole macrocycles delocalizes onto the fluorines. The DFT calculations described later in this paper appear to contribute some additional insights into this issue.

**Electrochemistry and XPS.** Figures 5 and 6 present the cyclic voltammograms of the new complexes described in this paper. Table 2 presents the half-wave potentials for one-electron oxidation and reduction of the Cu and FeCl $\beta$-octafluoro-*meso*-triarylcorroles, along with those of certain other relevant complexes. Despite the somewhat limited data set of four compounds, calculated Hammett $\rho$ values of substituent effects on the half-wave potentials are included in Table 2. The corresponding Hammet plots are shown in Figures S1 and S2 of the Supporting Information.

Table 2 shows that the half-wave potentials for one-electron oxidation of the Cu $\beta$-octafluoro-*meso*-triarylcorroles are positively shifted by approximately 400 mV, compared to their $\beta$-unsubstituted analogues. Interestingly, this positive shift due to $\beta$-octafluorination is identical to that previously observed for $\beta$-octabromination.[17] However, the Cu octafluorocorroles exhibit slightly higher half-wave potentials for reduction, i.e., are somewhat easier to reduce, than Cu octabromocorroles.[17]

The relatively high oxidation half-wave potentials of the fluorinated corroles are also consistent with the nitrogen 1s

***Table 2.*** Half-Wave Potentials, $E_{1/2}$ (V vs SCE) and Hammett $\rho$ Values (mV), for Cu, MnCl, FeCl and FeOFe Triarylcorroles in $CH_2Cl_2$ Containing 0.1 M TBAP

| compound | X subst. | 3$\sigma$ | $E_{1/2ox}$ | $E_{1/2red}$ | $\rho_{ox}$ | $\rho_{red}$ | ref |
|---|---|---|---|---|---|---|---|
| Cu[T(*p*-X−P)C] | $OCH_3$ | −0.80 | 0.65 | −0.24 | 95 | 68 | 17 |
| | $CH_3$ | −0.51 | 0.70 | −0.23 | | | |
| | H | 0 | 0.76 | −0.20 | | | |
| | $CF_3$ | 1.62 | 0.89 | −0.08 | | | |
| Cu[$Br_8$T(*p*-X−P)C] | $OCH_3$ | −0.80 | 1.10 | 0.04 | 58 | 86 | 17 |
| | $CH_3$ | −0.51 | 1.12 | 0.07 | | | |
| | H | 0 | 1.14 | 0.12 | | | |
| | $CF_3$ | 1.62 | 1.24 | 0.25 | | | |
| Cu[$F_8$T(*p*-X−P)C] | $OCH_3$ | −0.80 | 1.06 | 0.17 | 67 | 77 | this work |
| | $CH_3$ | −0.51 | 1.12 | 0.18 | | | |
| | H | 0 | 1.15 | 0.22 | | | |
| | $CF_3$ | 1.62 | 1.24 | 0.35 | | | |
| Mn[T(*p*-X−P)C]Cl | $CH_3$ | −0.51 | 0.97 | 0.07 | 82 | 77 | 24 |
| | H | 0 | 1.03 | 0.09 | | | |
| | $CF_3$ | 1.62 | 1.15 | 0.23 | | | |
| Fe[T(*p*-X−P)C]Cl | $CH_3$ | −0.51 | 1.02 | 0.03 | 74 | 77 | 24 |
| | H | 0 | 1.07 | 0.05 | | | |
| | $CF_3$ | 1.62 | 1.18 | 0.19 | | | |
| {Fe[T(*p*-X−P)C]}$_2$O | $CH_3$ | −0.51 | 0.59 | −0.35 | 114 | 109 | 24 |
| | H | 0 | 0.64 | −0.31 | | | |
| | $CF_3$ | 1.62 | 0.83 | −0.12 | | | |
| Fe[$F_8$T(*p*-X−P)C]Cl | $OCH_3$ | −0.80 | 1.34 | 0.47 | 49 | 68 | this work |
| | $CH_3$ | −0.51 | 1.38 | 0.48 | | | |
| | H | 0 | 1.40 | 0.49 | | | |
| | $CF_3$ | 1.62 | 1.47 | 0.63 | | | |

X-ray photoelectron spectra (XPS, Figure 7) of the free bases which show that the core ionization potentials of the protonated and unprotonated nitrogens of the fluorinated corroles are about 0.5 eV upshifted, relative to free-base octamethylcorrole [38,39] and 0.7 eV upshifted, relative to free-base tetraphenylporphyrin.[40,41] A detailed description of the XPS of various corrole derivatives prepared in our laboratory will be presented elsewhere.

In our previous work,[24,26] we have proposed that the oxidation half-wave potentials of metallocorroles serve as a probe of electronic character of the corrole ligand. This proposal was based on the observation that FeCl, MnCl, SnCl, and CrO corrole complexes generally exhibit higher oxidation half-wave potentials than analogous Cu, SnPh, FePh, and Fe−O−Fe complexes. We proposed that this indicates that the corrole ligands are substantially noninnocent (i.e., exhibit corrole $\pi$-cation radical character) in the former complexes while they are more innocent in the latter group of complexes.[26] The complexes reported here exhibit the same trend. Thus, the half-wave oxidation potentials of the FeCl $\beta$-octafluoro-*meso*-triarylcorroles are 230−270 mV higher than those of the corresponding Cu complexes, suggesting that in the FeCl $\beta$-octafluoro-*meso*-triarylcorrole complexes the corrole ligand is noninnocent. As before, we freely admit that this interpretation of the electrochemical results is speculative, but it is in agreement with the conclusions drawn on the basis of the NMR results.

A closer examination of the data in Table 2 allows us to engage in further speculation, vis-à-vis the electronic character of the fluorinated metallocorroles. In particular, we note that

(38) Licoccia, S.; Paolesse, R. *Struct. Bonding* **1995**, *84*, 71.
(39) Zanoni, R.; Boschi, T.; Licoccia, S.; Paolesse, R.; Tagliatesta, P. *Inorg. Chim. Acta* **1988**, *145*, 175.
(40) Gassman, P. G.; Ghosh, A.; Almlöf, J. *J. Am. Chem. Soc.* **1992**, *114*, 9990.
(41) Ghosh, A.; Moulder, J.; Bröring, M.; Vogel, E. *Angew. Chem., Int. Ed.* **2001**, *113*, 431.

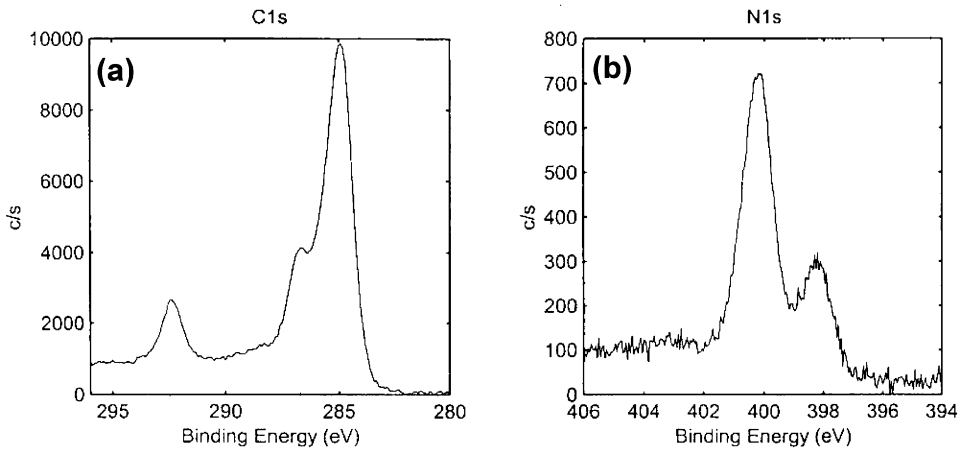


***Figure 7.*** (a) Carbon 1s and (b) nitrogen 1s XPS of $H_3[F_8T(p\text{-}CF_3\text{−}P)C]$. Note that the C 1s peak due to the $CF_3$ carbons is well-resolved at 292.5 eV. All of the β-octafluorocorroles also exhibit a resolved peak at 286.8 eV, which we assign to the fluorinated β-carbons.

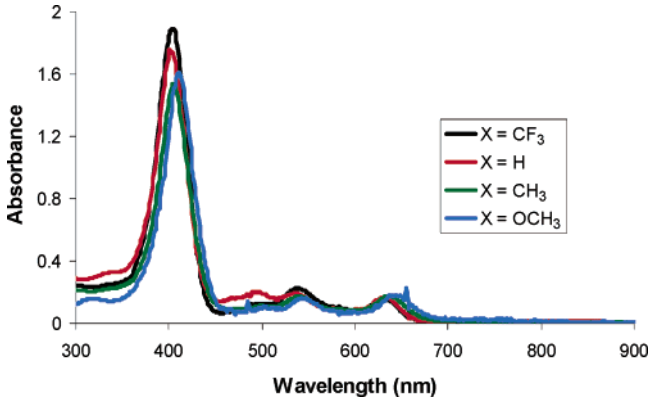


***Figure 8.*** UV−visible spectra of the free-base β-octafluoro-*meso*-tris(*p*-X-phenyl)corroles (X = $OCH_3$, $CH_3$, H, and $CF_3$) prepared in this work.

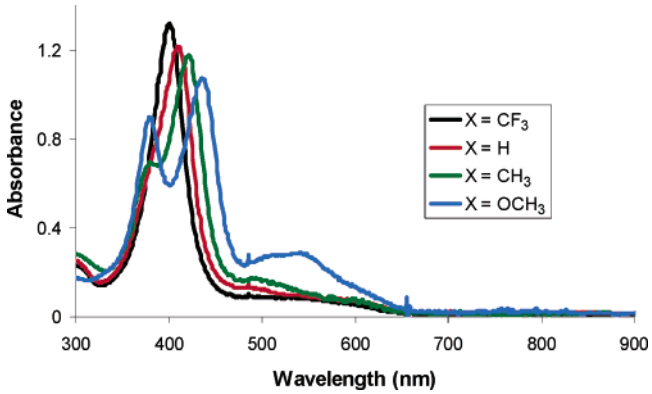


***Figure 9.*** UV−visible spectra of the Cu β-octafluoro-*meso*-tris(*p*-X-phenyl)corroles (X = $OCH_3$, $CH_3$, H, and $CF_3$) prepared in this work.

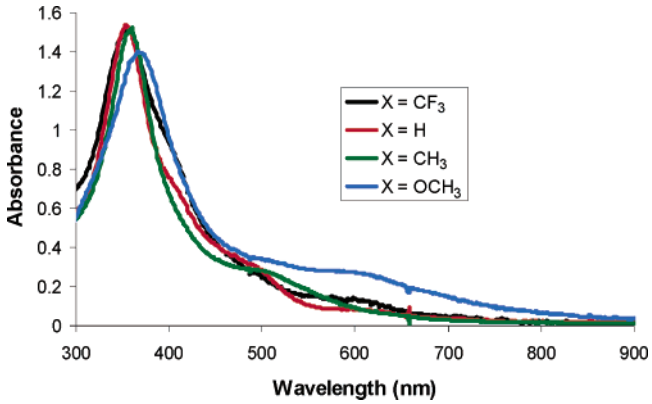


***Figure 10.*** UV−visible spectra of the FeCl β-octafluoro-*meso*-tris(*p*-X-phenyl)corroles (X = $OCH_3$, $CH_3$, H, and $CF_3$) prepared in this work.

the difference in the oxidation half-wave potentials between the FeCl and Cu corrole complexes ($E_{1/2(ox)}$(FeCl) − $E_{1/2(ox)}$(Cu)) decreases as the corrole ligand becomes more electron deficient. Thus, [$E_{1/2(ox)}$(FeCl) − $E_{1/2(ox)}$(Cu)] decreases in the following order: T(*p*-$CH_3$−P)C (315 mV) > TPC (308mV) > T(*p*-$CF_3$−P)C (288 mV) > $F_8$T(*p*-$OCH_3$−P)C (280 mV) > $F_8$T(*p*-$CH_3$−P)C (260 mV) > $F_8$TPC (250 mV) > $F_8$T(*p*-$CF_3$−P)C (230 mV). In other words, the oxidation half-wave potentials of the FeCl and Cu corrole complexes approach one another with increasing electron deficient character of the corrole ligand. We propose that this reflects the fact that a very electron-deficient ligand is always relatively innocent, regardless of the coordinated metal ion. Accordingly, for ligand-centered oxidation of such a ligand, different metal complexes should exhibit similar oxidation half-wave potentials.

The Hammett ρ (= (1/3)($dE_{1/2}/d\sigma$)) of 67 mV for the oxidation half-wave potentials of the Cu β-octafluoro-*meso*-triarylcorroles is considerably smaller than that for the corresponding unfluorinated Cu corroles, but similar in magnitude to that for Cu β-octabromo-*meso*-triarylcorroles (Table 2). As in the case of the Cu octabromocorroles,[17] we propose that the small Hammett ρ in this case reflects a HOMO switch among the three fluorinated Cu corroles studied, i.e., the more electron-rich Cu[$F_8$T(*p*-$OCH_3$−P)C], Cu[$F_8$T(*p*-$CH_3$−P)C], and Cu[$F_8$-TPC] may have a $b_1$ HOMO, whereas the more electron deficient Cu[$F_8$T(*p*-$CF_3$−P)C] may have an $a_2$ HOMO. It may be recalled that the corrole $a_2$ and $b_1$ HOMOs crudely resemble the $a_{1u}$ and $a_{2u}$ HOMOs of porphyrins, respectively.

**Electronic Absorption Spectra.** The electronic absorption spectra of the free-base, Cu, and FeCl β-octafluorocorrole derivatives are shown in Figure 8, 9, and 10, respectively. The Soret maxima are listed in Table 3, along with those of other relevant corrole derivatives. As observed for free-base *meso*-triarylcorroles which are not fluorinated at the β positions,[17,24] the Soret maxima of free-base β-octafluoro-*meso*-triarylcorroles are not particularly substituent-dependent. In contrast, the Soret maxima of the Cu β-octafluoro-*meso*-triarylcorroles red-shift strongly with increasing electron-donating character of the *para* substituents on the aryl group. The Soret maxima of the FeCl β-octafluoro-*meso*-triarylcorroles also red-shift somewhat in

***Table 3.*** "Soret" Band Maxima (nm) in $CH_2Cl_2$ for Some Relevant Triarylcorroles

| | substituent (X) | | | | | |
|---|---|---|---|---|---|---|
| corrole | *p*-$OCH_3$ | *p*-$CH_3$ | *p*-H | *p*-$CF_3$ | $F_5$ | ref |
| $H_3$[T(*p*-X−P)C] | 421 | 417 | 417 | 417 | 408 | 17 |
| Cu[T(*p*-X−P)C] | 433 | 418 | 413 | 407 | 406 | 17 |
| Cu[$Br_8$T(*p*-X−P)C] | 468 | 453 | 439 | 436 | 442 | 17 |
| Mn[T(*p*-X−P)C]Cl | | 441 | 433 | 423 | | 24 |
| Fe[T(*p*-X−P)C]Cl | | 421 | 411 | 402 | | 24 |
| {Fe[T(*p*-X−P)C]}$_2$O | | 389 | 385 | 384 | | 24 |
| $H_3$[$F_8$T(*p*-X−P)C] | 410 | 405 | 403 | 404 | | this work |
| Cu[$F_8$T(*p*-X−P)C] | 436, 380 | 421, 380 (sh) | 409 | 401 | | this work |
| Fe[$F_8$T(*p*-X−P)C]Cl | 367 | 360 | 355 | 353 | | this work |

response to *meso* substituents. As shown in Table 3, the substituent sensitivity seen for Cu $\beta$-octafluoro-*meso*-triarylcorroles has also been observed for Cu, FeCl, and MnCl complexes of $\beta$-unsusbstituted *meso*-triarylcorroles and also for Cu $\beta$-octabromo-*meso*-triarylcorroles. This phenomenon thus appears to be a fairly general feature of high-valent transition metal corrole complexes. We have ascribed these red shifts to significant charge transfer (CT) character in one or more electronic transitions in the Soret region.[17,24] DFT/CI and time-dependent DFT(PW91/TZP) calculations on gallium corrole ($C_{2v}$) and copper corrole ($C_{2v}$) revealed a number of CT transitions of high oscillator strength in the Soret region of Cu corrole, but not in the case of Ga corrole.[33] The CT transitions in the case of Cu corrole involve excitation into the LUMO, which is of $b_2$ symmetry and has predominant Cu($d_{x^2-y^2}$) character. The low-energy transitions of Ga corrole, in contrast, are all $\pi-\pi^*$ transitions.

**DFT Calculations.** Spin-unrestricted DFT (PW91/TZP) calculations on Cu $\beta$-octafluorocorrole shows that the S = 1 Cu(II) $b_1$ and $a_2$ radical states are only 0.11 and 0.19 eV, respectively, higher in energy than the S = 0 Cu(III) state. These results are qualitatively consistent with the temperature-dependent $^{19}$F spectra of the Cu corroles studied, which indicate the presence of a thermally accessible paramagnetic exited state. Perhaps not surprisingly, the low energies of the Cu(II) radical states are also consistent with what we found for $\beta$-unsubsituted Cu corrole, although this could not have been predicted a priori. In other words, $\beta$-octafluorination does not significantly effect the relative energetics of the Cu(III) versus the Cu(II) radical states.

Spin-unrestricted DFT (PW91/TZP) calculations on FeCl $\beta$-octafluorocorrole reveal a spin density profile (Figure 11) similar to the one calculated for the $\beta$-unsubstituted analogue.[24] Thus, the Fe and Cl atoms carry 1.91 and 0.21 $\alpha$ spins and the $\beta$-carbons carry a total of 0.12 $\alpha$ spins, respectively. In contrast, the *meso* carbons carry a total of 0.24 $\beta$ spins and the nitrogens a total 0.11 $\beta$ spins. The spatial distribution of the $\beta$ spins coincides precisely with the shape of the $b_1$ HOMO of the corrole ligand,[33] which crudely resembles the $a_{2u}$ HOMO of porphyrins. The overall spin density profile of this molecule, in particular the significant spatial separation of the $\alpha$ and $\beta$ spins, is further highly characteristic of antiferromagnetically coupled spin systems.[21,33,42,43] The antiferromagnetic coupling in FeCl $\beta$-octafluorocorrole seems to involve the metal center on one hand and the corrole $b_1$ HOMO on the other hand. An

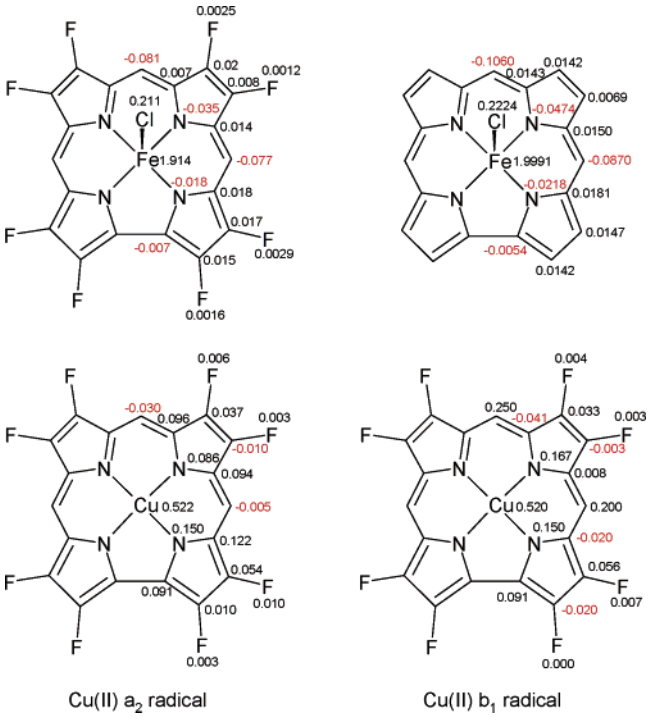


***Figure 11.*** Spin-unrestricted DFT(PW91/TZP) spin populations for FeCl $\beta$-octafluorocorrole and its $\beta$-unsubstituted analogue. Also shown are the spin populations of the Cu(II) $b_1$ and $a_2$ corrole radical states of Cu $\beta$-octafluorocorrole.

examination of the high-lying occupied MOs revealed an MO with a metal($d_{z^2}$)-corrole("$b_1$") overlap. This overlap is clearly facilitated by the significant displacements of 0.39 Å of the iron from the $N_4$ plane of the corrole in the optimized geometry. As in the case of the $\beta$-unsubstituted analogue,[24] these results are consistent with an electronic structure involving a corrole $\pi$ cation radical antiferromagnetically coupled to an intermediate spin (S = 3/2) Fe(III) center. The DFT calculations thus support the conclusions drawn from the electrochemical and NMR results.

A comparison of the spin density profile of the FeCl $\beta$-octafluorocorrole with the $\beta$-unsubstituted counterpart reveals that the *meso* carbons and nitrogens in the octafluorocorrole complex carry only about 80% of the $\beta$-spin found at the same positions in the $\beta$-unsubstituted complex (Figure 11). In other words, the octafluorocorrole ligands in the FeCl complexes are substantially noninnocent, but less so than their $\beta$-unsubstituted counterparts. This is consistent with the smaller isotropic shifts observed in the $^1$H NMR of the Fe[$F_8$T(*p*-X−P)C]Cl (X = $OCH_3$, $CH_3$, H, and $CF_3$) series compared to the Fe[T(*p*-X−P)C]Cl (X = $CH_3$, H, and $CF_3$) series (Table 1).

Finally, we make an attempt to relate the calculated spin density profile of FeCl $\beta$-octafluorocorrole with the $^{19}$F NMR spectra of the FeCl corroles studied. Figure 11 shows that all four symmetry-distinct $\beta$-fluorines carry small, positive spin densities, whereas the carbon−nitrogen skeleton of the corrole carries a net negative spin density. The fluorine spin densities

(42) Ghosh, A.; Vangberg, T.; Gonzalez, E.; Taylor, P. *J. Porphyrins Phthalocyanines* **2001**, *5*, 345.

(43) It should be noted that the PW91 functional used by us and the B3LYP functional used in ref 21 give qualitatively similar but, quantitatively, significantly different spin populations for FeCl corroles. In the absence of higher-level calculations of these results, we cannot say whether PW91 or B3LYP provide a better description of reality. For a review of calibration of PW91 and B3LYP calculations on biologically relevant transition metal complexes against CASPT2 and CCSD(T) calculations, see: Ghosh, A.; Taylor, P. R. *Curr. Opin. Chem. Biol.* **2003**, *7*, 113.

are too small to be taken at face value, but efforts are underway to verify the overall spin density profile with B3LYP and CASSCF calculations. Nevertheless, the fact that all the fluorine spin densities are small[44] and similar may be consistent with the observation that all the fluorines in a given FeCl octafluorocorrole derivative exhibit a narrow range of moderate isotropic shifts.

## Conclusions

The results presented in this paper lead to the following conclusions:

(1) The one-pot corrole synthesis first reported by the Gross[8,9] and Paolesse[10,11] groups in the late 1990s has evolved into a remarkably general and predictable self-assembly based synthetic reaction. In our hands, Gross's solvent-free procedure proved particularly effective and, in fact, more general than originally claimed. Thus, we showed that the reaction worked for a variety of aromatic aldehyde starting materials[17] and was not limited to relatively electron-deficient aldehydes, as in the original reports by Gross and co-workers.[8,9] Here, we have shown that the pyrrole component is also variable in that 3,4-difluoropyrrole undergoes oxidative condensation with four different aromatic aldehydes to yield β-octafluorocorroles.[19] We note that a variety of different substituted pyrroles have been synthesized in recent years such as 3,4-dimethoxypyrrole[45,46] and 3,4-bis(methylthio)pyrrole[47] and these have also been converted to the corresponding β-octasubstituted porphyrins.[47−49] We speculate that one-pot corrole syntheses should also be possible with a wide variety of different substituted pyrroles. Given that this synthesis may be viewed a seven-component self-assembly process, it is gratifying that it is robust with respect to significant variations in the electronic character of both the aldehyde and presumably also the pyrrole component.

(2) Electrochemistry and XPS have demonstrated the strongly electron-deficient character of the β-octafluorocorrole ligands. Thus, the XPS nitrogen 1s ionization potentials of these ligands are some 0.7 eV higher than those of the corresponding β-unfluorinated ligands. The oxidation half-wave potentials of the Cu and FeCl complexes of the fluorinated corroles are also positively shifted by 300−400 mV relative to their β-unsubstituted analogues.

(3) Various measurements on the compounds reported here throw considerable light on the nature of high-valent transition metal compounds and of noninnocent ligands. Thus, $^1$H NMR spectroscopy suggests that the new β-octafluorinated triarylcorroles act as substantially noninnocent ligands, i.e., exhibit corrole π-cation radical character, in the FeCl complexes. Quantitatively, however, NMR spectroscopy and DFT calculations indicate that the β-octafluorocorrole ligands are less noninnocent than the corresponding β-unsubstituted triarylcorrole ligands in their FeCl complexes. We have argued, albeit less rigorously, that our electrochemical results also support this picture.

(4) It is gratifying that the FeCl complexes exhibit broad but distinctively discernible $^{19}$F NMR peaks. The peaks exhibit significant but by no means enormous isotropic shifts which may reflect that the highly electronegative fluorine atoms carry only relatively small spin densities, i.e., relatively little of the π-cation radical character of the corrole macrocycles delocalizes onto the fluorines.

(5) The $^{19}$F NMR of the Cu complexes exhibit two relatively broad peaks that sharpen at lower temperature, and we propose that this is indicative of a thermally accessible Cu(II) corrole π-cation radical excited state. There is thus a tendency toward noninnocent corrole ligands for the copper complexes studied, even though a diamagnetic Cu(III) ground state is the overwhelmingly dominant species between −40 and 40 °C.

(6) We have previously reported that the electronic absorption spectra, particularly the Soret absorption maxima, of high-valent transition metal triarylcorroles are very sensitive to the nature of the substituents at the *meso* positions. In contrast, the Soret absorption maxima of free-base triarylcorroles are not particularly sensitive to the nature of the *meso* substituents. The same scenario holds for the fluorinated corroles described here. Thus, while the three free-base fluorinated triarylcorroles exhibit practically identical Soret absorption maxima, the Soret bands of the Cu derivatives of the same corroles red-shift by approximately 35 nm on going from the *p*-$CF_3$ to the *p*-$OCH_3$ derivatives. Theoretical calculations suggest that these red shifts result from significant charge-transfer character in one or more transitions in the Soret region.

**Acknowledgment.** This work was supported by the VISTA program of Statoil (Norway) as well as by the Norwegian Research Council. We thank Prof. F. Ann Walker for her detailed comments on the manuscript, a number of constructive suggestions related to the NMR studies, and a preprint of ref 21.

**Supporting Information Available:** DFT optimized Cartesian coordinates and $^1$H NMR, $^1$H$^1$H COSY, $^{19}$F NMR, and resonance Raman spectra (PDF). This material is available free of charge via the Internet at http://pubs.acs.org.

JA021158H

(44) In an early DFT study (Ghosh, A. *J. Am. Chem. Soc.* **1995**, *117*, 4691) of porphyrins, one of us noted that *meso*- and β-halogen substituents exert quite different electronic effects. In particular, *meso*-halogen substituents strongly stabilize porphyrin A2u radicals, presumably by absorbing some spin density from the meso positions. A similar situation might be operative for *meso*-fluorinated corroles, which are unknown so far.

(45) Merz, A.; Schwarz, R.; Schropp, R. *Adv. Mater.* **1992**, *4*, 409.
(46) Merz, A.; Meyer, T. *Synthesis* **1999**, 94.
(47) Sugiura, K.-i.; Kumar, M. R.; Chandrashekar, T. K.; Sakata, Y. *Chem. Lett.* **1997**, 291.
(48) Merz, A.; Schropp, R.; Lex, J. *Angew. Chem., Int. Ed. Engl.* **1993**, *32*, 293.
(49) Merz, A.; Schroppe, R.; Doetterl, E. *Synthesis* **1995**, *7*, 795.